Chapter IV

Ionic contribution to the Dielectric Properties of Nematic Liquid Crystals in Thin Cells

4.1 Introduction

In the previous chapter we have discussed the effect of confinement on the order parameters of some nematic liquid crystals. It is found that the order parameters in thin cells in all the compounds with aromatic cores are enhanced significantly with respect to those in thick cells. The Landau de Gennes theory partially accounts for the enhancement of order parameter in thin cells if the surface potential is sufficiently strong.

In this chapter we will discuss the effect of confinement on the dielectric properties of a nematic liquid crystal in thin cells.

Liquid crystals are dielectric materials. However, due to ionic impurities, they usually have nonzero values of conductivity σ. Unless special precautions are taken σ can be ~10^{-9} $(\Omega\text{-cm})^{-1}$ [1]. The dielectric constant is written as a complex quantity, $\varepsilon^* = \varepsilon' - j\varepsilon''$, where ε' is the real part of the dielectric constant and ε'' is the dielectric loss factor of the medium, with $j = \sqrt{-1}$. The dielectric dispersion spectrum of a nematic liquid crystal depends on the direction of the applied field with respect to the director ($\hat{n}$). When $\vec{E} \parallel \hat{n}$, the relaxation frequency comes down to fairly low values (a few KHz to a few MHz depending on the material and the temperature). For $\vec{E} \perp \hat{n}$, the relaxation frequency is in the GHz range. At very low frequencies ($\leq$ 1KHz), the ionic impurity also contributes to the dielectric properties. The influence of ions on the real and imaginary parts of the complex dielectric constant of both solid and liquid electrolytes has been studied both experimentally and theoretically for a long time [2-4]. The theory has since been extended for polymer melts [5], which was subsequently simplified to describe the ionic effect on the dielectric response of the isotropic (I) phase of liquid crystals [6-9]. These experiments were performed on liquid crystal cells with thickness of

about 5μm or larger. In view of the emerging interest in using much thinner cells in LCDs, as well as due to an intrinsic interest in the problem we carried out dielectric investigations on liquid crystal cells with thicknesses < 2μm. When the thickness is reduced, at any given voltage the field increases and the influence of the ions on the electrical properties becomes significant. The earlier studies on the ionic contribution were made for describing electro-hydrodynamic instabilities (EHD), and also on the dc switching process in a boundary layer bistable nematic display [10-12]. In display devices, the liquid crystal is usually aligned with its director parallel to the glass plates. The dielectric anisotropy ($\Delta\varepsilon$) of the material is positive so that the nematic shows a realignment of the director above a threshold voltage [1] (Freedericksz transition). We have chosen a material with negative dielectric anisotropy to avoid such a problem. However, such a material can give rise to EHD instabilities beyond a threshold of about ≈ 5V or more, depending on the frequency [1]. We conducted our experiments at 1V, which is well below the threshold value. In this chapter we will describe both the experimental and theoretical results on the frequency dependence of the dielectric properties on a nematogen which exhibits the nematic phase in a wide temperature range.

4.2 Experimental

The compound studied is 2-cyano 4-heptylphenyl-4'-pentyl-4-biphenyl carboxylate [7(CN)5] which has the following phase sequence: Cr 45 ^{0}C N 102 ^{0}C I. The chemical structure of the molecule is shown in Fig.(4.1). In the previous chapter we have reported the measurement of birefringence in thin and thick cells of this compound. The lateral cyano group of the molecule gives rise to a negative dielectric anisotropy in the nematic phase. The material has a very wide nematic range and it can be supercooled down to room temperature. It is also chemically stable. The cells are prepared as mentioned before (see Fig.(1.16) in chapter-I. A heating stage (INSTEC HS1) is used to control the temperature to an accuracy of ~10mK. The dielectric properties of the cells are measured using a DSP lock-in amplifier (SRS 830). The block diagram of the experimental setup is shown in Fig.(4.2).

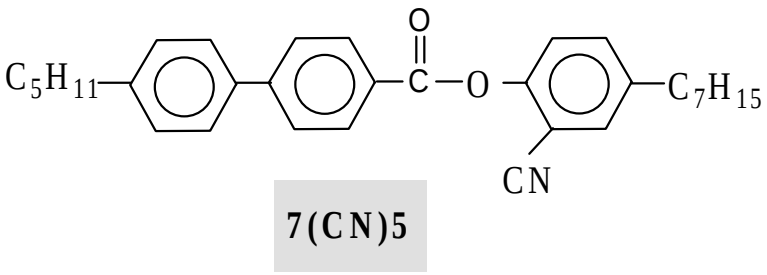

Figure 4.1: Molecular structure of the compound 7(CN)5 used in the experiment.

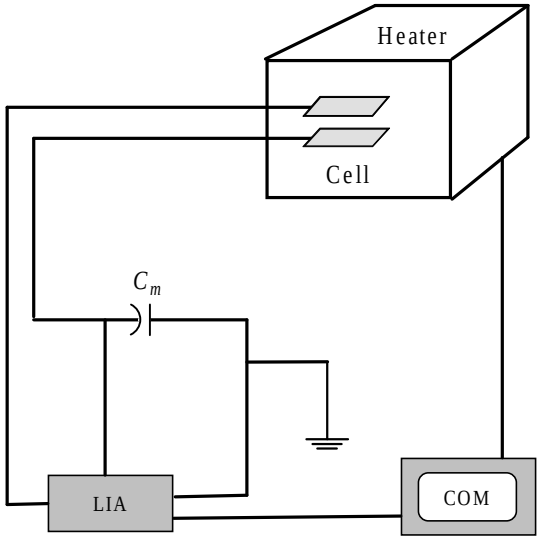

Figure 4.2: Block diagram of the experimental setup. Lock-in amplifier (LIA), Capacitor (C_m), Computer (COM).

The sinusoidal output of the internal oscillator of the lock-in amplifier is adjusted to an r.m.s. value of V_0 = 1V, and applied to the cell which is in series with a $1\mu F$ standard capacitor (C_m).

4.3 Equivalent Circuit and Impedance Analysis

As mentioned in chapter–II, we consider the sample cell to be electrically equivalent to a resistor and a capacitor in parallel (see Fig.(4.3)). We measure the amplitude and phase of the voltage developed across a series capacitance, C_m (=1μF), which is large in comparison to the capacitance of the sample cell (~150 pF). It is important that C_m is large so that the maximum voltage drop is across the cell and only a

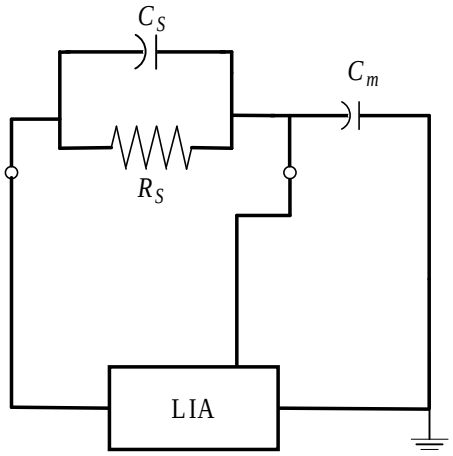

Figure 4.3: Equivalent circuit used for the impedance analysis of the liquid crystal cell. C_S and R_S are the sample capacitance and resistance respectively.

small voltage is measured by the LIA. The impedance of the modelled cell is given by

$$Z_c = R_S \frac{\left(1 - j\omega C_S R_S\right)}{\left(1 + \omega^2 C_S^2 R_S^2\right)} \tag{4.1}$$

where R_S and C_S are the sample resistance and capacitance. $\omega = 2\pi f$ where f is the frequency of the applied voltage. The total impedance of the circuit Z_T, which is a series combination of Z_c and $1/j\omega C_m$ is given by

$$Z_T = \frac{\omega R_S C_m - j\left(1 + \omega^2 R_S^2 C_S \left(C_m + C_S\right)\right)}{\omega C_m \left(1 + \omega^2 C_S^2 R_S^2\right)}. \tag{4.2}$$

The total current flowing through the circuit is given by

$$I_T = \frac{V_0 e^{j(\omega t + \phi_0)}}{Z_T}$$

where V_0 and ϕ_0 are the amplitude and phase of the output voltage of the LIA. Substituting Z_T in the above equation we get

$$I_T = \frac{V_0 e^{j(\omega t+\phi_0)} \omega\, C_m \left(1+\omega^2 C_S^2 R_S^2\right)}{\omega R_S C_m - j\left(1+\omega^2 R_S^2 C_S \left(C_m + C_S\right)\right)}. \tag{4.3}$$

The voltage drop across C_m, which is measured by LIA is given by

$$V_m e^{j(\omega t+\phi_m)} = I_T Z_m \tag{4.4}$$

where $Z_m = 1/\left(j\omega\, C_m\right)$ and V_m and ϕ_m are the amplitude and phase of the measured signal. Simplifying the above expression by separating the real and imaginary parts we get the following relations for the resistance and capacitance of the sample [13]

$$R_S = \frac{Y}{\omega \sin\alpha}$$

$$C_S = \frac{X}{Y}, \tag{4.5}$$

where $X = \cos\alpha - Q$, $Y = \frac{\sin^2\alpha + X^2}{C_m Q}$, $Q = \frac{V_m}{V_0}$ and $\alpha = \phi_0 - \phi_m$. The calibration of the setup was checked by connecting standard capacitors in parallel with standard resistors in place of the liquid crystal cell. It was found that the stray capacitance is ~2 *pF*. The accuracy of the measured capacitance is ~1% and that of the resistance is ~3%. We have also checked the calibration by measuring the capacitance and resistance using a Wayne-Kerr bridge which operates at 1.6 KHz. The measurements were controlled by a computer using suitable programs. The measurements were made at several frequencies in the range of 10-1100 Hz.

4.4 Experimental Results and Discussion

In order to bring out the strong influence of the cell thickness on the measured properties, we have shown the effective dielectric constant [which is the ratio of the cell capacitance with the sample (C_S) to that of the empty cell] and conductivity at 1.1 KHz as functions of temperature for both the cells in Fig.(4.4) and Fig.(4.5), respectively. The effective conductivity is given by

$$\sigma_{\perp} = d \big/ (aR_S) \tag{4.6}$$

where *a* is the electrode area. These measurements correspond to $\varepsilon_{\perp}$ and $\sigma_{\perp}$, where the subscript refers to the direction in relation to the director. In Fig.(4.4), the dielectric constant measured in the 6.7μm thick cell follows the expected trend, decreasing with increase of temperature, the rate of decrease becoming rapid near the nematic-isotropic transition point T_{NI}. It is easily shown that [1] the contribution from the liquid crystal is given by

$$\varepsilon_{\perp} = \bar{\varepsilon} - \frac{1}{3}\Delta\varepsilon_0 S \tag{4.7}$$

where $\bar{\varepsilon} = (\varepsilon_{\parallel} + 2\varepsilon_{\perp})/3$ is the average dielectric constant, and $\Delta\varepsilon_0$ is the value of the dielectric anisotropy when the order parameter S=1. As S decreases with increase of temperature, and $\Delta\varepsilon_0$ is negative, $\varepsilon_{\perp}$ decreases with temperature. The trend shown by the thin cell is peculiar. The dielectric constant is somewhat larger than that for the thicker cell even at low temperatures, but at temperatures above 60 ^{0}C, the value does not decrease as in the thicker cell but more or less remains constant and decreases slightly only very near T_{NI}. In both cases, the dielectric constant jumps to a lower value at T_{NI}. Further, the value of ε measured in the thinner cell continues to be significantly larger than that for the thicker one even in the isotropic phase.

The variations of $\sigma_{\perp}$ for both the cells are shown as functions of temperature in Fig.(4.5). As expected, the conductivity increases with temperature in both cases as the mobility and the number density of the ions increase with temperature. However, it can be noted that the relative variation of $\sigma_{\perp}$ in the thin cell is somewhat higher than that in the thick cell.

The markedly different response of the thin cell compared to the thick one arises due to the ionic contribution. In order to investigate this effect in greater detail, we have carried out frequency dependent measurements of the dielectric properties at different temperatures.

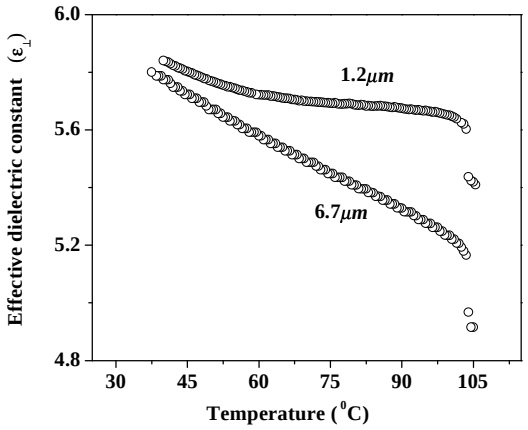

Figure 4.4: Temperature dependences of the effective dielectric constant of the liquid crystal taken in cells with two different thicknesses, at a frequency of 1.1KHz. Note the higher value for the thinner cell, which hardly varies with temperature in the nematic phase above 60 ^{0}C.

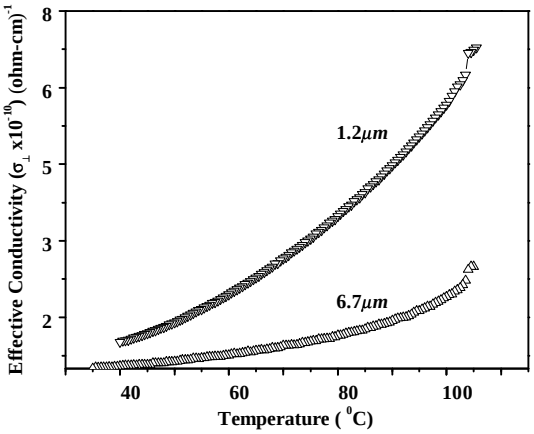

Figure 4.5: Temperature dependences of the effective conductivity of liquid crystal in the two cells as described in the caption of Fig.(4.4).

The raw data on the effective dielectric constant and the conductivity are not convenient for a comparison with the theoretical analysis to follow. We first present a summary of the theoretical background.

4.4.1 Theoretical Analysis

The liquid crystal is separated from the ITO electrodes by aligning polyimide layers as in LCDs. This boundary layer has a typical thickness of few hundred $\overset{0}{A}$ and its effective electrical resistance (R_{bl}) as well as capacitance (C_{bl}) can be expected to be quite large, i.e. the layers are essentially insulating. As the dielectric constant of this layer is similar to that of the liquid crystal, it can be assumed that there is no absorption of ions at the interface between the two. The dielectric constant ($\varepsilon_{\perp}$) of the liquid crystal medium itself, which depends on the induced dipole moment and orientation polarisation contributions of the molecules can be considered to be essentially frequency independent in the range (<1.2 KHz) in which the measurements have been made. This contribution produces an effective bulk capacitance denoted by C_B. The medium also has a uniform distribution of ions, which produces a frequency independent conductivity σ, which in turn produces a bulk resistance of the medium denoted by R_B. The application of an electric field generates a non-uniform distribution of ions, which depends on the frequency and in turn contributes both to the real and imaginary parts of the dielectric constant. These in turn give rise to a capacitance $C_I(\omega)$ and resistance $R_I(\omega)$. The equivalent circuit corresponding to the cell in which all these contributions have been included is shown in Fig.(4.6).

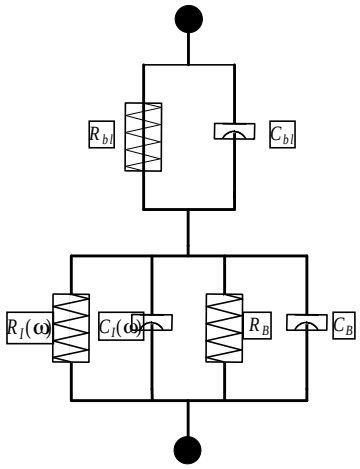

Figure 4.6: Equivalent circuit of the liquid crystal cell with the “lumped” values of the boundary layer capacitance C_{bl} and resistance R_{bl} arising from both the boundaries.

The complex impedance of the equivalent circuit is given by [6]

$$Z_A = \frac{2R_{bl}}{1+(\omega R_{bl}C_{bl})^2} + \frac{\dfrac{1}{R_B}+\dfrac{1}{R_I(\omega)}}{\left[\dfrac{1}{R_B}+\dfrac{1}{R_I(\omega)}\right]^2 + \omega^2[C_B + C_I(\omega)]^2} - j\left[\frac{2\omega {R_{bl}}^2 C_{bl}}{1+(\omega R_{bl}C_{bl})^2} + \frac{\omega[C_B + C_I(\omega)]}{\left[\dfrac{1}{R_B}+\dfrac{1}{R_I(\omega)}\right]^2 + \omega^2[C_B + C_I(\omega)]^2}\right]. \quad (4.8)$$

In terms of the measured values C_S and R_S [given by equation (4.1)], the measured complex impedance is given by

$$Z_B = \frac{R_S}{1+(\omega R_S C_S)^2} - j\left[\frac{\omega {R_S}^2 C_S}{1+(\omega R_S C_S)^2}\right]. \quad (4.9)$$

We summarise below a grossly simplified method of evaluation of the ionic contribution which generates $C_I(\omega)$ and $R_I(\omega)$. It is convenient to assume that positive ions are very much more mobile than the negative ones and the latter do not contribute to the current. If ρ (z,t) is the charge density of the mobile ions, the charge continuity equation is given by

$$\frac{\partial \rho(z,t)}{\partial t} + \frac{\partial J(z,t)}{\partial z} = 0 \quad (4.10)$$

where J(z,t) is the current density, which is given by

$$J(z,t) = -D\frac{\partial \rho(z,t)}{\partial z} + \mu\rho(z,t)Ee^{j\omega t} \quad (4.11)$$

where D is the diffusion coefficient and μ is the mobility. As the polyimide is a blocking layer, we can assume that at the two boundaries (z = 0 and d), J_0=J_d=0. As our measurements have been made only at the frequency ω of the applied voltage, we assume that

$$\rho(z,t) = \rho_0(z) + \rho_1(z)e^{j\omega t} \quad (4.12)$$

where $\rho_0(z)$ is the time independent density of ions and $\rho_1(z)$ is the amplitude of ion density which oscillates at the frequency of the applied field. The mobile charges move

under the action of the external field and the resulting space charges produce a polarisation which contributes to the total dielectric constant. The space charges give rise to a non-uniform electric field, which can be calculated by using the Poisson relation. The solutions in that case are quite complicated and can not be expressed in a simple analytical form. Our sample had unknown ionic species whose number density (n) is ~10^{15} /cc. As such, the sample is really a *weak* electrolyte. Furthermore, the transit time of the ions from one electrode to the other under a reversal of voltage V is given by $\tau_{tr} = (6\pi\eta r/q)(d^2/V)$ where η, the coefficient of viscosity is ≈1 poise at room temperature, and r the ionic radius can be expected to be ~$10\,\overset{0}{A}$. However as the mesogenic molecules are strongly polar we can also expect that the ion will be dressed by a few molecules which are attached to the ion. The effective "ionic" radius can be a few (say~5) times larger than the bare value. For the thick cell (~7μm), $\tau_{tr} \approx 2\,\mathrm{s}$ while it is about 0.1s for the thinner one (~1.5μm) for the applied voltage of 1V. As such, in the frequency range of interest (10-1100 Hz), to a good approximation, the non-uniformity in ion distribution can be assumed to be small. The electric field in the cell then can be assumed to be equal to the external field. As the temperature is increased, the viscosity reduces and the approximation becomes less justifiable. However use of the approximation has the virtue that analytical expressions can be derived for $C_I(\omega)$ and $R_I(\omega)$. In a recent paper Sawada et al [7] have also argued that the approximation may be adequate. Moreover, we can fit the experimental data quite well to the solutions by using this approximation, which is hence further justified *a posteriori.* Using the boundary condition that J=0 it can be shown that ρ_0 is actually independent of z and

$$\rho_1(z) = \frac{\mu E}{\kappa D}\rho_0\left(\frac{e^{\kappa z}}{1+e^{\kappa d}} - \frac{e^{-\kappa z}}{1+e^{-\kappa d}}\right) \qquad (4.13)$$

where $\kappa = \sqrt{j\omega/D}$ and from the Einstein relation, $\mu/D = q/k_BT$, where k_B is the Boltzman constant. Hence $\rho_1(z)$ has components both in phase and $\pi/2$ out of phase with the applied A.C. field. Taking D = 2.5×10^{-8} cm^2/sec (see Table-I), E = 30esu, the

calculated variation of the real part of $\rho_1(z)$ is shown in Fig.(4.7) in the $1\mu m$ thick cell at a temperature of 65 ^{0}C.

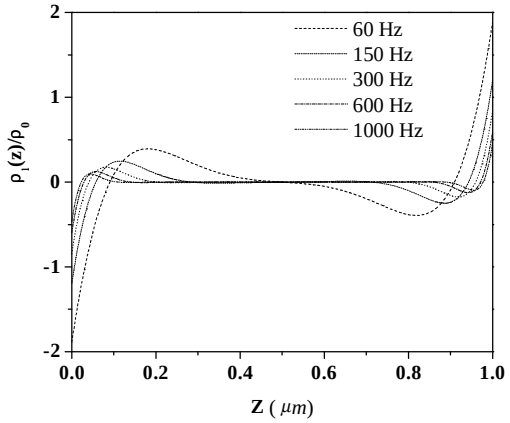

Figure 4.7: Variation of $\rho_1(z)/\rho_0$ inside the thin cell ($1\mu m$) as a function of *z* at the temperature of 65^{0}C.

It is noticed that the space charge density is higher at lower frequencies (for example at 60 Hz) in the bulk as well as near the surfaces. With increasing frequency the space charge density is reduced in the bulk as well as near the surfaces. Therefore at lower frequencies the space charge effect is dominant. The additional polarisation due to the space charge formation is $[\rho_1(z)z]$ and the thickness-averaged value is

$$\overline{P}(t) = e^{j\omega t}\frac{\int_0^d z\rho_1(z)dz}{\int_0^d dz} \tag{4.14}$$

The corresponding frequency- dependent ionic contributions to the complex dielectric constant are given by:

$$\frac{C_I(\omega)d}{\varepsilon_0 a} = \varepsilon_I'(\omega) = -\left[\frac{4\pi n q^2 D}{\omega k_B T A}\right]\left[\frac{1+2e^A\sin(A)-e^{2A}}{1+2e^A\cos(A)+e^{2A}}\right] \tag{4.15}$$

and

$$\frac{d}{\omega\varepsilon_0 R_I(\omega)a} = \varepsilon_I''(\omega) = \frac{4\pi n q^2 D}{\omega k_B T}\left[1+\frac{1-2e^A\sin(A)-e^{2A}}{A\left(1+2e^A\cos(A)+e^{2A}\right)}\right] \tag{4.16}$$

where "*a*" is the area of electrodes, $nq = \rho_0$ and $A = d\sqrt{\omega/2D}$. Equation (4.15) and (4.16) agree with those derived by Sawada [6]. Using these in equation (4.8), the real and imaginary parts of Z_A can now be calculated. Comparing them with the corresponding parts of the experimental complex impedance Z_B given by equation (4.9), a nonlinear least-squares fitting procedure (Levenburg –Marquet) is used to get the best values for R_{bl}, C_{bl}, D, n and the frequency independent terms R_B and C_B. Some representative variations of the real and imaginary parts of the impedance are shown in figures (4.8-4.13) at three different temperatures for both the thin and thick samples. It is seen that the agreement between the calculated and the measured variations is quite satisfactory. The relevant fit parameters at different temperatures are collected in Table-I for both the thin and thick samples. From the figures it is clear that the real part of Z_B, which gives the experimental data has a monotonic decrease as a function of frequency at all temperatures for the cells of both thicknesses. The calculated values, which are the real part of Z_A agree well with the data. The imaginary part of (the measured) Z_B, and the corresponding calculations based on Z_A, show a peak around 100 Hz, which is more pronounced for the thin cell (Fig.(4.9)). The frequency corresponding to the peak decreases as the temperature is lowered, while the magnitude of the impedance

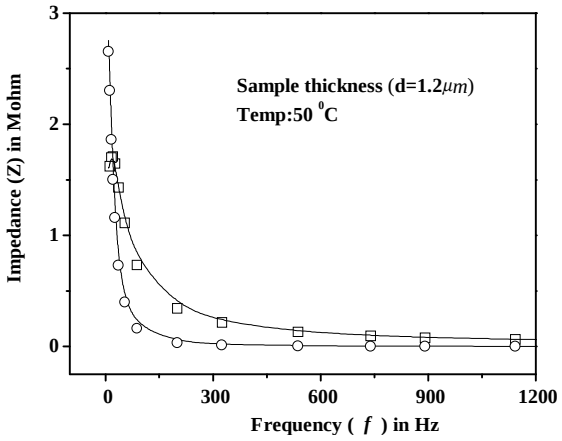

Figure 4.8: Temperature dependences of the real (open circles) and imaginary (open squares) parts of the measured impedance Z_B [see equation (4.9)] in the cell with thickness 1.2μm, at 50 ^{0}C. the lines show the calculated variations of Z_A [see equation (4.8)] with the fit parameters shown in Table-Ia.

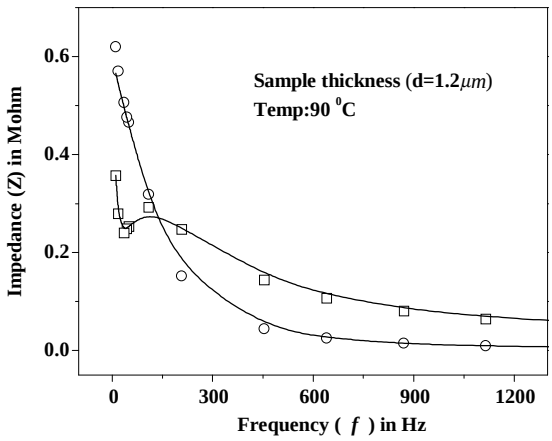

Figure 4.9: Same as in Fig.(4.8), at a temperature of 90 ^{0}C. Note the minimum and the maximum in the frequency dependence of the imaginary part of the impedance.

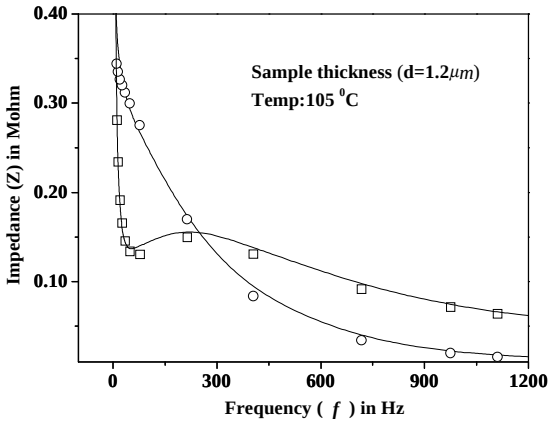

Figure 4.10: Same as in Fig.(4.9), at a temperature of 105^{0}C. Note the minimum and maximum in the frequency dependence of the imaginary part of the impedance.

itself increases. In the thin cell there is also a low frequency minimum above 75 ^{0}C and the impedance strongly increases at very low frequencies. The physical origin of these features can be understood from equations (4.8), (4.9), (4.15) and (4.16). $A = d\sqrt{\omega/2D}$,

i.e., $A \alpha f^{1/2}$ where $f = \omega/2\pi$ and the lowest frequency f that we have used is 10 Hz. As the typical diffusion constant D~10^{-7} cm^2/s, A is much larger than 1 even for the thin cell. The boundary layer capacitance C_{bl} is $\approx 10^{-7} F$, and the corresponding resistance R_{bl} $\approx 10^7 \Omega$. Using these, the imaginary part of Z_A can be approximated to $Z_A(imag) \approx \frac{C_1}{\omega} + \frac{C_2 \omega}{\left(1 + C_3 \omega^2\right)}$, where C_1~10^7, C_2~10^4 and C_3 ~10^{-6}. It is clear that the second term leads to a maximum when $\omega^2 = 1/C_3$ where $\sqrt{C_3}$ is essentially the charge relaxation time $\varepsilon_0 \varepsilon_\perp / \sigma$. On the other hand, C_1 arises from the boundary layer impedance and the first term becomes comparable to the second one for $\omega \approx 100$ Hz (i.e., $f \approx 20$ Hz). Below this frequency the contribution from the boundary layer leads to a rapid increase in $Z_A(imag)$ and hence produces the sharp minimum seen in Fig.(4.9).

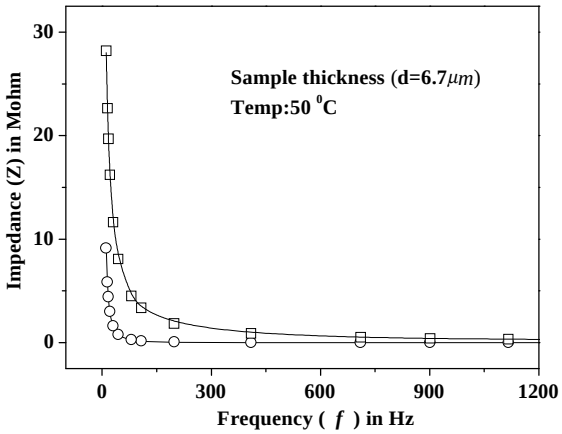

Figure 4.11: Temperature dependences of the real (open circles) and imaginary (open squares) parts of the measured impedance Z_B [see equation (4.9)] in the cell with thickness 6.7μm, at 50 ^{0}C. The lines show the calculated variations of Z_A [see equation (4.8)] with the fit parameters shown in Table-Ib.

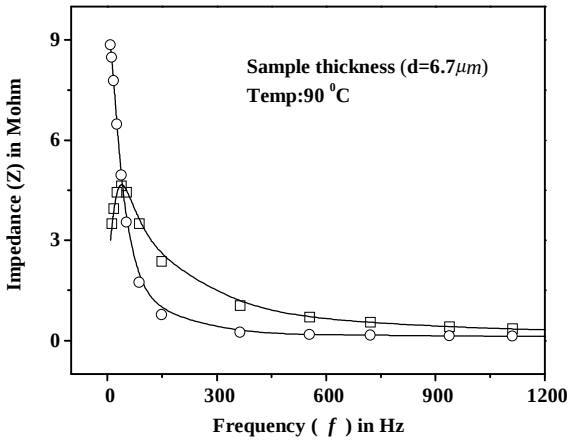

Figure 4.12: Same as in Fig.(4.11) at 90^0C. Note the peak in the frequency dependence of the imaginary part of the impedance.

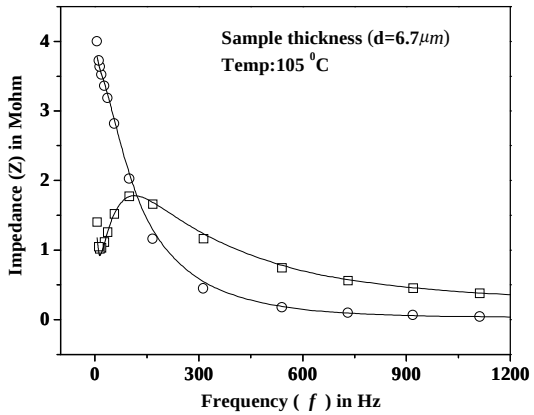

Figure 4.13: Same as in Fig.(4.12) at 105 ^{0}C. Note the peak in the frequency dependence of the imaginary part of the impedance.

From Table-I, the number density of ions at any given temperature is much larger in the thin cell compared to the thick one, which arises due to the fact that the two cells were prepared on different days and the contamination during processing of the cells is likely to be responsible for the different values. One can assume that the bulk conductivity $\sigma \approx \mu\rho$ and the values of the bulk resistivity R_B are consistent with the

Table-Ia
Fit parameters at different temperatures

(a) Sample thickness d=1.2μm

Temperature in ^0C	Diffusion Constant D (cm^2/sec) in ($\times 10^{-8}$)	Number Density ($n/c.c$) ($\times 10^{14}$)	Boundary Layer Resistance R_{bl} (in *Mohm*)	Boundary Layer Capacitance C_{bl} ($\times 10^{-7}$ F)	Bulk Resistance R_B in *Mohm*	Bulk Capacitance C_B ($\times 10^{-9}$ F)
105	6.3	20	7	2.7	1.5	2.1
90	4.9	16	7	2.7	3.4	2.1
65	2.5	6.6	7	2.7	3.2	2.2
50	1.9	4.5	7	2.7	8.5	2.4

Table-Ib

(b) Sample thickness d = 6.7μm

Temperature ^{0}C	Diffusion Constant D (cm^2/sec) ($\times 10^{-8}$)	Number Density ($n/c.c$) ($\times 10^{14}$)	Boundary Layer Resistance R_{bl} in *Mohm*	Boundary Layer Capacitance C_{bl} ($\times 10^{-8}$ F)	Bulk Resistance R_B in *Mohm*	Bulk Capacitance C_B ($\times 10^{-10} F$)
105	9.7	4.8	12	9	12	3.8
90	8.8	2.5	12	9	50	4.15
65	6.1	0.6	12	9.01	83	4.4
50	5.4	0.2	13	9.0	145	4.71

diffusion constant D and the number density n in both the cells. Both decrease as the temperature is lowered as expected. The bulk value C_B is proportional to $\varepsilon_\perp$, the dielectric constant of the liquid crystal. From independent measurements [14] $\varepsilon_\perp \approx 5$ in the compound used in the present study and decreases with increase of temperature as required by equation (4.7). On the other hand, the boundary layer values R_{bl} and C_{bl} which are the lumped values from the polyimide coatings on both the electrodes hardly vary with temperature.

It is also easy to understand the higher effective dielectric constant exhibited by thin cells compared to the thick one (Fig.(4.4)). The ions move faster under the higher field acting in the thin cell, and also as the transit distance is shorter, the space charge contribution to the polarisation is relatively large. Consequently, the effective dielectric constant goes up. This is reflected in equation (4.15) in which $A \propto d$ occurs in the denominator of the expression for $\varepsilon'_I(\omega)$. From that equation, the ionic contribution is also $\propto nD^{3/2}$. As the number density as well as the diffusion coefficient increase with temperature (see Table-Ia), $\varepsilon'_I(\omega)$ increases with temperature, and compensates for the decrease of $\varepsilon_\perp$ with temperature reflecting that of the order parameter S as given by equation (4.7). The consequence is that the effective dielectric constant remains practically independent of temperature over a wide range [see Fig.(4.4)].

4.5 Conclusions

Our experiments have shown that as the thickness of the cell is reduced to ~1-2 μm, the ionic contribution to the dielectric response of a liquid crystal cell can be significant for samples with a conductivity ~$10^{-10}(\Omega\text{-cm})^{-1}$. The effect grows very large [$\propto \omega^{-3/2}$ for the real part and $\propto \omega^{-1}$ for the imaginary part, see equations (4.15) and (4.16)] as the frequency is reduced. In our simplified analysis, we have used the approximation that the non-uniformity of the electric field inside the cell arising from space charges can be ignored. The resulting simplified expressions for $\varepsilon'_I(\omega)$ and $\varepsilon''_I(\omega)$ reproduce the experimental data semi-quantitatively even for the thin cell at high temperatures. Liquid crystals which are used in very thin display devices have to be highly purified to avoid the ionic contribution to the dielectric response and hence to the

electrooptic characteristics. The non-uniform field arising from the space charge effects can be expected to alter the Freedericksz threshold voltage for materials with positive dielectric anisotropy. This might partially account for the large increase in the Freedericksz threshold voltage in thin cells compared to that in the thick cells, (see section 3.3) which can not be explained on the basis of the increase in order parameter in the thin cells.

References

[1] P.G. de Gennes and J. Prost, "The Physics of Liquid Crystals.," 2nd ed. (Claredon, Oxford, 1993).

[2] G. Jaffe, " Theory of Conductivity of semiconductors.," Phys. Rev. **85**, 354 (1952).

[3] R. J. Friauf, "Polarisation effect in the ionic conductivity of silver bromide.," J. Chem. Phys. **22**, 8 (1954).

[4] J. R. Macdonald, " Theory of ac space charge polarisation effect in photoconductors, semiconductor and electrolytes.," Phys. Rev. **92**, 1 (1953).

[5] S. Umera, "Ionic contribution to the complex dielectric constant of a polymer under dc bias.," J. Polym. Sci. **10**, 2155 (1972).

[6] A. Sawada, K. Tarumi, and S. Naemura, " Effect of electric double layer and space charge polarisation by plural kinds of ions on complex dielectric constant of liquid crystal materials.," Jpn. J. Appl. Phys., Part-1 **38**, 1418 (1999).

[7] A. Sawada, H. Sato, A. Manabe, and S. Naemura, " Study of internal electric field of liquid crystal cell effected by space charge polarisation.," Jpn. J. Appl. Phys. Part 1 **39**, 3496 (2000).

[8] A. Sawada,Y Nakazono, K. Tarumi and S. Naemura, “Complex dielectric constant of liquid crystal materials containing ionic impurities in low frequency region.,” Mol. Cryst. Liq. Cryst., **318**, 225 (1998).

[9] A. Sawada, k. Tarumi and S. Naemura, “ Novel characterisation method of ions in liquid crystal materials by complex dielectric constant measurements.,” Jpn. J. Appl. Phys, **38**, 1423 (1999).

[10] T. Z. Qian, Z. L. Xie, H. S. Kwok and P. Sheng, “ Dynamic flow and switching bistability in twisted nematic liquid crystal cell.,” Appl. Phys. Lett. **71**, 596 (1997).

[11] J. X. Guo and H. S. Kwok, “ High performance transmitive bistable twisted nematic liquid crystal displays.,” Jpn. J. Appl. Phys, Part1 **39**, 1210 (2000).

[12] R. N. Thurston, J. Cheng, R. B. Mayer, and G. D. Boyd. “Physical mechanism of dc switching in a liquid crystal bistable boundary layer display.,” J. Appl. Phys. **56**, 263 (1984).

[13] G. Bassapa and N. V. Madhusudana, “Effect of strong electric fields on the phase transitions in some liquid crystals.,” Mol. Cryst. Liq. Cryst. **288**, 161 (1996).

[14] B. S. Srikanta and N.V. Madhusudana, “Effect of skewed cybotactic structure on the dielectric constants and conductivities of some binary mixtures exhibiting the nematic phase.,” Mol. Cryst. Liq. Cryst. **103**, 111 (1983).